JACS
JOURNAL OF THE AMERICAN CHEMICAL SOCIETY

Article

pubs.acs.org/JACS

Probing the Unique Dehydration-Induced Structural Modifications in Cancer Cell DNA Using Surface Enhanced Raman Spectroscopy

Sajanlal R. Panikkanvalappil, Megan A. Mackey, and Mostafa A. El-Sayed*

Laser Dynamics Laboratory, School of Chemistry and Biochemistry, Georgia Institute of Technology, Atlanta, Georgia 30332-0400, United States

Supporting Information

ABSTRACT: Conformation-induced formation of a series of unique Raman marker bands in cancer cell DNA, upon dehydration, have been probed for the first time with the use of surface enhanced Raman spectroscopy (SERS). These bands are capable of distinguishing cancer cell DNA from healthy cell DNA. For this simple and label-free DNA detection approach, we used conventional spherical silver nanoparticles, at a high concentration, without any aggregating agents, which gave highly reproducible SERS spectra of DNA separated from various human cells irrespective of their highly complex compositions and sequences. The observed phenomenon is attributed to the change in the chemical environment due to the presence of nucleobase lesions in cancer cell DNA and subsequent variation in the nearby electronic cloud during the dehydration-driven conformational changes. Detailed analysis of the SERS spectra gave important insight about the lesion-induced structural modifications upon dehydration in the cancer cell DNA. These results have widespread implications in cancer diagnostics, where SERS provides vital information about the DNA modifications in the cancer cells.

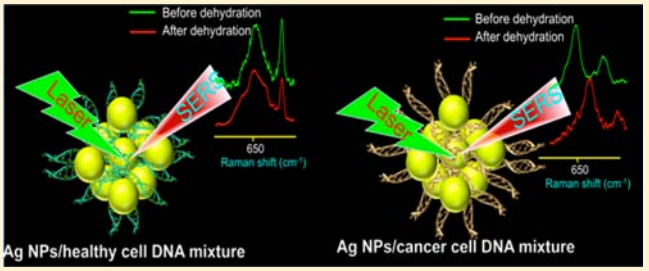

1. INTRODUCTION

Identification of genetic modifications in cancer cells is becoming increasingly imperative in the treatment of cancer, as successful treatments heavily depend on early detection of the disease. The continuous exposure of the cellular constituents to chemical carcinogens, ionization radiations, reactive oxygen species (ROS), and so forth could potentially result in irreversible modifications to the genetic material,[1,2] which may ultimately result in genomic mutations and cancer.[3] Chemical modification of DNA has been recognized as the most important epigenetic change in carcinogenesis, and elevated levels of oxidative DNA lesions have been noted in many tumors, strongly implicating the vital role of such damage in the origin of cancer.[4,5] Since these modifications are at the molecular level, precise detection of these events requires an ultrasensitive tool. Even though there are several reports on promising methods for monitoring structural modifications in DNA,[6,7] they exhibit some drawbacks, as they require expensive and complex enzyme-based target or signal-amplification procedures. Nanomaterial-based detection techniques have received keen attention, as it is a safe and reliable way to detect cancer in a simpler and relatively inexpensive way even at the very earliest stages.[8−10] Surface enhanced Raman spectroscopy (SERS)[11,12] is a powerful spectroscopic technique, offering several important advantages in medical diagnostics. It is a noninvasive and highly sensitive analytical tool, capable of providing structural fingerprinting of analytes.[13−16] The SERS phenomenon is also capable of detecting various structural, thermodynamic, and kinetic properties of DNA and is not limited by the size or state of aggregation.[17−19] Apart from the molecular information, they give an insight to various electrostatic, hydrophobic, and hydrogen bonding interactions between the nucleotides.[20−24]

Many current SERS-based DNA detection methods focus on the identification of modifications in model synthetic DNA systems such as nucleic acid bases, their modified forms, and some of the single- and double-stranded nucleotides.[25,26] Although Raman spectroscopy has been widely used for the identification of cancer biomarkers and DNA modifications[27−29] in vitro and in vivo, attaining reliable and precise information regarding chemically modified base lesions present in cancer cell DNA is still a difficult task, as only subtle modifications will be present in malignant DNA compared with nonmalignant DNA bases. As a result, a SERS-based method to detect chemical modifications in DNA and RNA qualitatively and quantitatively still remains a challenge. Nevertheless, SERS being a powerful analytical tool, variations in the chemical environments and associated modifications in the molecular vibrations in DNA can be precisely detected. We have extended our interest in finding out such Raman marker bands in cancer cells by using SERS. Here, for the first time, we traced a series of unique conformation-induced formations of DNA Raman marker bands in cancer cell DNA during its dehydration-driven structural transformation, making it possible to distinguish them from the healthy cells with the help of SERS.

Received: January 7, 2013
Published: March 7, 2013

dx.doi.org/10.1021/ja400187b | J. Am. Chem. Soc. 2013, 135, 4815−4821

2. EXPERIMENTAL SECTION

2.1. Preparation of Ag@Citrate. Citrate capped silver nanoparticles (Ag@Citrate) were prepared according to a previously reported procedure.[30] Briefly, to a boiling solution of 5 mM solution of silver nitrate in 50 mL deionized water, 75 mg of sodium citrate dissolved in 1 mL deionized water was added dropwise, and heating was continued further for a few minutes. The solution turned light yellow in color, indicating the formation of nanoparticles. The suspension was cooled in an ice bath. Later, 10 mL of the as-prepared Ag@Citrate solution was centrifuged, and the precipitate was washed with distilled water to remove excess citrate. Finally, the precipitate was dissolved in 500 μL of deionized water. The concentration of this solution was denoted as "*X*". These nanoparticles show surface plasmon resonance peak at 420 nm, which is characteristic of silver nanoparticles.

2.2. Cell Culture. Human oral squamous carcinoma cells (HSC-3) and human keratinocytes (HaCaT) were maintained in Dulbecco's modified Eagles' medium (DMEM, Mediatech) supplemented with 10% v/v fetal bovine serum (FBS, Mediatech) and 1% antimycotic solution (Mediatech) in a 37 °C, 5% CO_2 humidified incubator.

2.3. UV Irradiation Procedure. HSC-3 and HaCaT cells were grown in 12-well tissue culture plates overnight. For homogeneous irradiation of cells, the 12-well tissue culture plate was placed 1.5 cm under a UVC light source (254 nm, 1.12 mW/cm^2) for 1 h. Following irradiation, the cells were harvested by trypsinization and centrifugation for further analysis.

2.4. DNA Isolation. Genomic DNA was isolated by using an extraction procedure described earlier.[31,32] Briefly, the cells were lysed with 4 mL of lysis buffer containing 0.5 M Tris-HCl (pH 8.0), 20 mM EDTA, 10 mM NaCl, 1% SDS, and 0.5 mg/mL proteinase K. This was incubated overnight at 55 °C. Subsequently, 2 mL of saturated NaCl (~6 M) was added, and the samples were incubated at 55 °C for 10 min. After centrifugation at 5000 rpm for 30 min, the supernatant containing DNA was mixed with 2 volumes of prechilled ethanol (100%), and the DNA was spooled by gently inverting the mix. The tubes were incubated at room temperature for 15 min and recovered the DNA by centrifuging at 10 000 rpm for 10 min at room temperature. The DNA was washed several times thoroughly with 70% ethanol. The tubes were placed inverted on benchtop and allowed to air-dry at ambient condition. The required amount of DNA was dissolved in deionized water and was immediately used for the SERS analysis.

2.5. Oxidation of DNA using Fenton's Reagent. Oxidation of the DNA was carried out by treating it with Fenton's reagent.[33] Briefly, DNA isolated from HaCaT cells were solubilized in deionized water to a concentration of 0.1 mg/mL. Reaction mixtures containing 2 mL of DNA and Fenton's reagent (25 μM of Fe^{2+} and 0.03% of H_2O_2) were incubated at 37 °C for 1 h by gentle shaking. The reaction was terminated by adding 5 M NaCl to a final concentration of 1 M followed by 2 volume of prechilled ethanol. The solution was placed at −20 °C for 2 h and the precipitated DNA was separated by centrifugation at 10 000 rpm for 10 min. The DNA pellet was washed with 70% ethanol, dried in air and solubilized using required amount of water prior to the SERS measurements. Similar experiment was conducted with double stranded (ds) DNA of sequence 5′-AAGCGCGCGCGCTT-3′ (this sample is named as "AAG"). For the comparative study, we also used another dsDNA (5′-AATATATATATATATT-3′), which does not have any guanine base (this is named as "AAT"). All of the synthetic DNA samples were purchased from Sigma-Aldrich, U.S.

2.6. SERS Measurements. For the SERS studies, 2 μL of DNA (1 mg/1 mL) solution mixed with 2 μL of Ag nanoparticle solution (concentration "*X*") was used. This DNA-Ag colloid mixture solution was placed on a Si wafer. All of the SERS spectra were measured with an 1800 lines/mm grating using a Renishaw InVia Raman spectrometer (with a spectral resolution of ~1 cm^{-1}) coupled to a Leica microscope. The laser (532 nm) was directed into a microscope via a series of reflecting lenses and apertures, where it was focused onto the sample by a 50× objective. The backscattered signals from the samples were collected by a CCD detector in the range of 400 to 2000 cm^{-1}. The spectra were processed by removal of the spectral background. Here, cubic spline interpolation is used for the baseline fit by manually selecting the points representative of the background.

3. RESULTS AND DISCUSSION

With oxidative damage to DNA being responsible for many genomic mutations and carcinogenesis, the specific goal of this investigation was to identify DNA mutations in cancer cells using SERS. Human DNA consists of millions of nucleotides[34] and it has been shown that DNA can adopt random orientations on the metal surfaces.[35] Keeping this in mind, the first step in this work was to optimize the experimental conditions in order to obtain characteristic and reproducible SERS spectra from the DNA extracted from malignant and healthy cells. In order to get reliable spectra of the DNA, we used a concentrated silver nanoparticle (AgNP) solution (details about the concentrations have been given later) for the SERS measurements to ensure the nucleobases present will be in close proximity to the SERS hot spots within the AgNP clusters (Figure 1A). A marked difference in the reproducibility

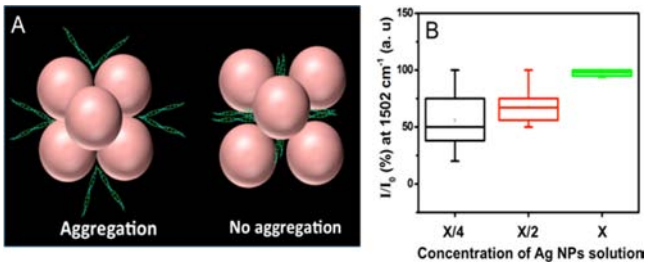

Figure 1. (A) Schematic representation of the interaction of DNA with AgNPs in aggregated and nonaggregated states. (B) Ratios of intensities of Raman lines correspond to 1502 cm^{-1} in healthy cell DNA, plotted as a function of AgNP concentration.

of Raman signal intensity was observed upon increasing the concentration of AgNPs (Figure 1B). Here, 10 mL of the as-prepared nanoparticles were centrifuged and the AgNP pellet was dispersed in 500 μL deionized water (concentration *X* in Figure 1B). This solution was further diluted by 2 and 4 times with deionized water (concentrations *X*/2 and *X*/4, respectively in Figure 1B). As seen in Figure 1B, the intensity of Raman signal at 1502 cm^{-1}, selected for the comparison, was highly fluctuating at a lower AgNP concentration (*X*/4), while nearly 100% reproducibility was achieved when the highest concentration (*X*) was used. This clearly shows that the concentration of AgNPs is a crucial component in SERS measurements of the DNA polymer. The reproducible signal, even after 10 consecutive measurements, suggests that the interaction of DNA with the AgNPs does not result in any structural modification to the DNA and the aggregation of Ag nanoparticles. Absence of any drastic change in the absorption maximum of the AgNPs after the addition of DNA also confirms this (see Supporting Information 1). We did not use any aggregating agent so that the interparticle spacing between adjacent nanoparticles were preserved to a greater extent which can accommodate more number of DNA strands.

The high concentration of nanoparticles virtually acts as aggregated nanoparticles, which are known to enhance the intensity of Raman vibrations by the enhanced electric field created by the gap in between the nanoparticles.[36,37] The significant enhancement in the SERS signal of DNA could be

attributed to the fact that the higher density of AgNPs in the 3D volume (Figure 1A) could allow excitation of a larger number of NPs by the laser thereby molecular vibrations of the DNA constituents. Whereas, in presence of an aggregating agent (0.1 M $MgSO_4$) the Raman spectra were inconsistent and the intensity ratios between the SERS bands were fluctuating, which restricted us to get the exact information on the changes in the SERS bands (Supporting Information 2). Apart from this, addition of metal ions can induce the aggregation of DNA and corresponding modifications in their conformations.[29b]

The effectiveness of highly concentrated nanoparticle solution in enhancing the Raman signals of the analyte molecule has been further verifyed by measuring the SERS spectra from a solution containing methylene blue (MB) of concentration 10^{-8} M at different nanoparticle concentrations (X, $X/2$, $X/3$, and $X/4$). A considerable increase in the intensity of Raman vibrations has been observed as the nanoparticle concentration increased (see Supporting Information 3). This was comparable to the SERS enhancement found when $MgSO_4$ (0.1 M) is used as an aggregating agent (see Supporting Information 4). This validates our argument that highly concentrated AgNPs solution resembles to the aggregated nanoparticles. We noticed that the intensity ratios between the Raman bands and the reproducibility of the SERS spectra were considerably enhanced when silicon wafer was used instead of the glass substrates (see Supporting Information 5). This could possibly be due to the fact that the hot spots created in between the AgNPs could strongly couple and interconnect by the semiconducting Si wafers, which can lead to an enhancement in the electric field around the Ag NPs.[13b] Also, a variation in the Raman vibration frequency of DNA backbone is expected since the reorientation of the phosphate groups due to the involvement of hydrogen bonding between phosphate group in the DNA with silanol group in glass.

Commonly, DNA damage is caused by the attack of ROS and subsequent conformational changes of DNA domains on the nanometer scale; monitoring these transformations is of considerable interest in cancer diagnostics. In the SERS spectrum, the region 600−1200 cm^{-1} can give significant information about the structural modifications in DNA since it is designated as ring breathing (RB) vibrations of purine or pyrimidine residues, as well as stretching of bonds within the backbone deoxyribose ring.[38] A slight modification in the glycosyl torsion angle and/or deoxyribose ring pucker may affect the intensity and peak position of Raman vibrations in the DNA molecule,[39] allowing for the identification of oxidatively damaged malignant DNA.

Interested in detecting the extent of oxidative damage in human cells, we analyzed the DNA extracted from various cell lines using SERS. The SERS measurements were done by drop casting a 1:1 mixture of AgNP/DNA solution onto a Si wafer (see Experimental Section). The spectra were collected by focusing the laser directly onto the solution as a function of time upon dehydration. SERS spectra of DNA extracted from HaCaT and HSC-3 cells collected at 5 min intervals. Closer examination of the spectra revealed several unique modifications in the Raman features of certain vibrations in the HSC-3 cell DNA. Among them, the Raman vibration corresponding to the guanine RB mode of the HSC-3 cell DNA dramatically changed upon dehydration, compared with that of HaCaT cell DNA. Figure 2A,B shows an expanded view of the SERS spectra corresponding to the guanine RB vibration of HaCaT and HSC-3 cell DNA, respectively (full spectra are given in

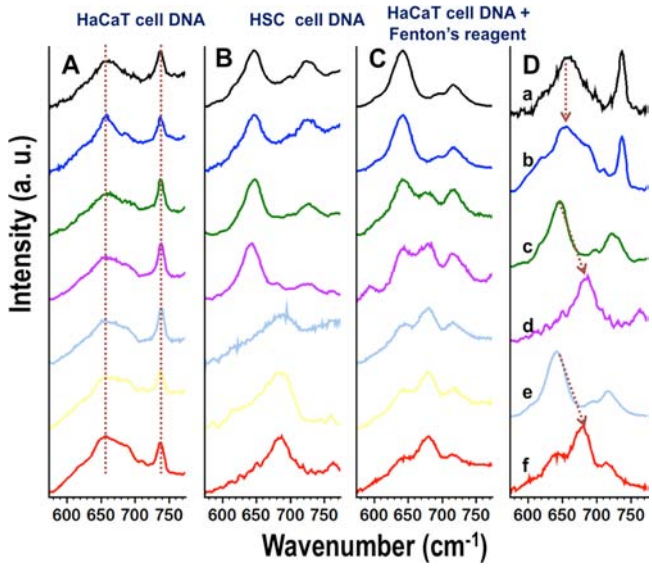

Figure 2. Time-dependent SERS spectra collected as a function of water evaporation (top to bottom; 0−30 min; 5 min intervals) showing guanine RB mode of healthy (A) and cancer cell DNA (B), as well as the healthy cell DNA treated with Fenton's reagent (C). (D) SERS spectra corresponding to guanine RB mode of various DNA samples collected upon dehydration as a function of time: (a,b) healthy cell DNA (0 and 30 min, respectively), (c,d) cancer cell DNA (0 and 30 min, respectively), (e,f) healthy cell DNA treated with Fenton's reagent (0 and 30 min, respectively).

Supporting Information 6). HaCaT cell DNA, exhibits guanine RB band at ∼660 cm^{-1}, while it is found at ∼640 cm^{-1} in HSC-3 cell DNA. Normally, the RB frequency of guanine varies from 600 to 700 cm^{-1}, depending on the sugar-base conformation.[40] Upon dehydration (up to 20 min), a new conformation-sensitive Raman band (∼675 cm^{-1}) emerged for HSC-3 cell DNA. This clearly indicates the modification in the conformation of DNA upon dehydration. The formation of the new Raman band in the HSC-3 cell DNA is shown in Figure 2B. Under identical conditions, this band was not found in the healthy cell DNA (Figure 2A), although the RB band of guanine became broader and a shoulder band appeared at ∼680 cm^{-1}, which implies the absence of any major base lesion-induced modification in the HaCaT cell DNA.

It is well-known that carcinogenesis is prominently associated with DNA damage, especially via nucleobase lesions formed by ROS. One of the most common DNA lesions, and therefore an important biomarker of oxidative damage, is 8-oxoguanosine.[41−43] We propose a few reasons for the observed dramatic shift in the Raman band corresponding to the guanine RB mode upon evaporation of water from the cancer cell DNA. The interaction of water molecules with DNA is known to be a powerful influence on its conformation.[44−46] The hydration shell present around DNA is mainly dependent on the relative humidity,[47] such that DNA in aqueous solution predominantly exists in its B form, but deviates from this conformation upon dehydration.[48] The presence of lesions in the DNA can induce kinks in the backbone. This could modify the electron cloud and the extent of interaction between DNA and water molecules. Compared to native guanine, 8-oxoguanine has a high hydrogen bond occupancy, due to the interactions of O8 and H7 with water.[49] The oxygen molecule attached to C8 in 8-oxoguanine can act as a new hydrogen acceptor, and hydrogen attached to N7 can function as a hydrogen donor (Figure

dx.doi.org/10.1021/ja400187b | J. Am. Chem. Soc. 2013, 135, 4815−4821

3A,B). Mutagenicity of oxoguanine has been attributed to its ability to attain syn and anti conformations, relative to the

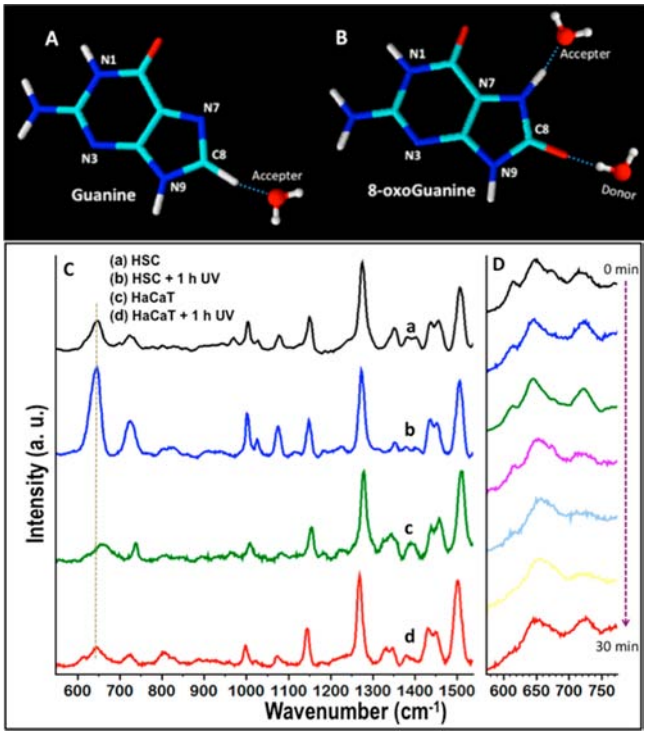

Figure 3. Schematics showing interactions of water molecules with guanine (A) and 8-oxoguanine (B). (C) SERS spectra of healthy and cancer cell DNA before and after irradiation to UVC light (254 nm for 1 h). (D) SERS spectra showing the RB vibration of guanine in healthy cell DNA exposed to UVC radiation. Spectra were collected as a function of time (top to bottom; 0−30 min; 5 min intervals) during dehydration of the DNA.

glycosidic bond of the deoxyribose sugar and their chance to form stable Watson−Crick pair as well as Hoogsteen mispairs.[50] Thermodynamic studies show that oxoguanine destabilizes DNA by reducing the enthalpy.[51] Oxidation of guanine modifies the DNA backbone torsional angle distributions to a certain extent.[45] As a result, the environment around an oxoguanine-cytosine base pair is fundamentally different from that of the native guanine-cytosine. Hence, a profound difference in the hydration shell can be observed around a DNA lesion, which can modify the electron cloud in the vicinity of lesion sites.

The electron cloud can be further modified by any small variation in the hydration shell. Dehydration of the DNA solution and the possible conformational transformation from the B-form could also modify the electronic environment. This effect would be prominent in cancer cell or oxidized DNA, as more amounts of lesions are likely to be present in these cases.

The dramatic shift observed in the guanine RB band in oxidized and cancer cell DNA can possibly be due to the large shift in the electronic environment during dehydration. It has been shown that guanine prefers the anti conformation, whereas 8-oxoguanine prefers to adopt the syn conformation in DNA.[50,52] The 8-oxo group in oxidized guanine creates a steric repulsion with the deoxyribose O4′ oxygen atom in the anti conformation.[52] The frequency of RB vibration could also be modified by the coupling of the low frequency of the guanine RB mode with bond stretching vibrations of the furanose ring. Thus, the extent of base-sugar coupling will be greater in the lesion containing DNA. This can also contribute to the modification of the environment near the lesion sites, thereby leading to the change in Raman vibrations during dehydration.

In order to investigate how Raman bands are affected by the oxidation of DNA by interaction with ROS, we performed a control experiment where the DNA collected from healthy cells were oxidized by treatment with Fenton's reagent. Of the ROS, the highly reactive hydroxyl radical (•OH) formed during the reaction can easily attack the double bonds of DNA bases and form many lesions, especially 8-oxoguanine.[53] Here, the DNA was treated with Fenton's reagent for about 60 min and the SERS spectra were collected at different time intervals during dehydration (Figure 2C). SERS full spectra are given in the Supporting Information 7. The SERS spectra showed a similar trend as in the case of cancer cell DNA. After the oxidation of the healthy cell DNA, via Fenton's reagent, the Raman band corresponding to the RB mode of guanine shifted from 660 to 640 cm^{-1}. Note that the RB mode for cancer cell DNA was also observed at around 640 cm^{-1}. This suggests that the cancer cell DNA may also contain oxidized base lesions, which are responsible for the shift in the RB vibration compared to healthy cell DNA. The shift in the RB band can be attributed to the increased presence of 8-oxoguanine in cancer cell DNA and their high hydrogen bond occupancy compared to native guanine. In order to check this, we measured the SERS spectra of guanosine (dG) and 8oxo-guanosine (8-oxo-dG). We found that RB vibration of dG found at 675 cm^{-1} shifted toward lower wavenumber side and appeared at 642 cm^{-1} in the 8-oxo-dG (see Supporting Information 8).

Due to the possibility of this extended hydrogen bonding, the vibrational motions of nucleotides in the cancer cell DNA are greatly influenced by their local interaction strength, as well as geometries and dynamics. The kink in the DNA backbone at the lesion site can reduce the force constant of bending, which ultimately reflects in the frequency of Raman vibrations, as seen with the shift in the RB band of guanine. The extent of shift can also act as a measure of oxidative stress. Similar to the cancer cell DNA, the RB band of the healthy cell DNA, observed at 640 cm^{-1}, gradually disappeared upon dehydration and a new band appeared at 682 cm^{-1}. This clearly indicates a modification in the conformation of DNA by the interaction with ROS generated during the Fenton's reaction. The abstraction of a hydrogen atom from the deoxyribose moieties of DNA by ROS can lead to single-strand breaks. Radical attack on the bases also results in the addition of a hydroxyl group to the electron-rich N7−C8 bond in purines and 5,6 bonds in the pyrimidines.[54] This can modify the environment around the lesion sites, the extent of interaction with water molecules, and the conformation of DNA.

It was noted that the RB band corresponding to adenine, found at 738 cm^{-1}, remained almost the same for the healthy cell DNA even at 30 min of dehydration. In contrast, the cancer cell DNA exhibited a band at 727 cm^{-1}, which nearly disappeared after dehydration. Due to the presence of oxoguanine there is a possibility of local collapse of the B conformation in the cancer cell DNA. This can induce a strong repulsive electrostatic interaction between oxoguanine and neighboring nucloetides at lesion sites, which can lead to the flipping of adenine on the complementary strand.[55] The abundance of oxidized base lesions in the cancer cell may enhance this process. During dehydration and subsequent

dx.doi.org/10.1021/ja400187b | J. Am. Chem. Soc. 2013, 135, 4815−4821

conformational change, the RB band corresponding to adenine may be red-shifted and merged with the modified guanine band, which appeared at ~675 cm^{-1}.

To look at the the phenomenon of dehydration induced conformational changes and related modifications in the Raman features, SERS experiments for small chain length DNA have been conducted before and after treatment with Fenton's reagent (Figure 4). For this study, dsDNA-AAG was used. The

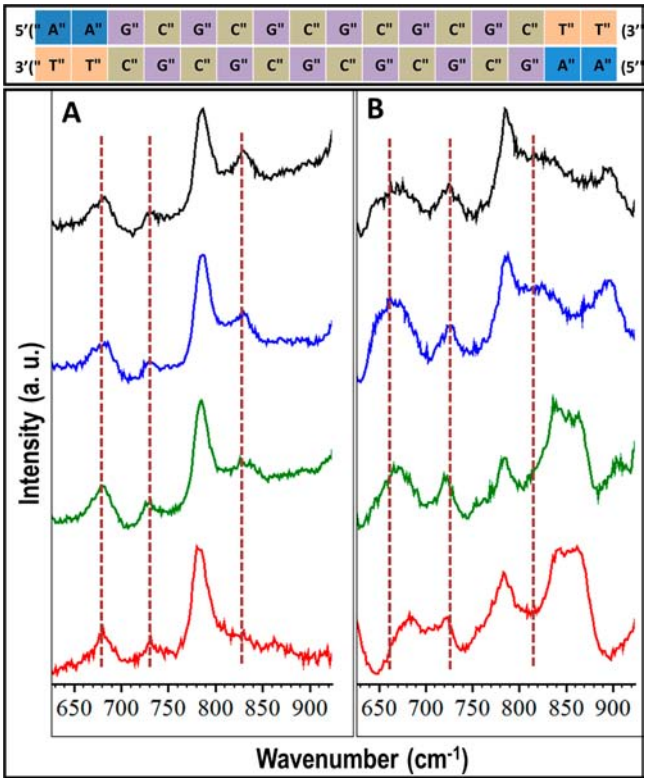

Figure 4. Time-dependent SERS spectra collected as a function of water evaporation (top to bottom; 0–30 min; 10 min intervals) showing guanine RB mode of dsDNA-AAG before (A) and after (B) treatment with Fenton's reagent. The DNA sequence of dsDNA-AAG is given at the top.

RB vibration of guanine was prominent (681 cm^{-1}) in the SERS spectrum [this was absent in the dsDNA-AAT which does not contains any guanine residue (Supporting Information 8)]. Upon treatment with Fenton's reagent, the guanine RB vibration found at 681 cm^{-1} in dsDNA-AAG was shifted to 662 cm^{-1}. Similar shift was also observed in the HSC cell DNA in comparison with HaCaT cell DNA. Apart from this, RB vibration of guanosine shifted toward a higher wavenumber side (from 662 cm^{-1} to 682 cm^{-1}) was also found in the Fenton's reagent treated dsDNA-AAG upon dehydration, although it was not as prominent as in cancer cell DNA (Figure 4B). However, this was absent in the DNA before treatment with the same (Figure 4A). This suggests that other factors such as presence of nucleobase lesions other than oxoguanine and DNA fragement size may also contribute to the formation of new Raman bands during dehydration induced conformational changes. This confirms our argument that the presence of base lesion is indeed involved in the formation of the unique Raman bands in cancer cell DNA upon dehydration. The stretching vibrations, corresponding to the backbone phosphodiester marker band in dsDNA-AAG increased in its intensity upon dehydration after treatment with Fenton's reagent and shifted from 820 to ~850 cm^{-1} (Figure 4B). Similarly, the RB vibration due to adenine showed a nominal shift from 727 to 723 cm^{-1} upon dehydration in oxidized DNA.

It is important to understand whether all of the structural modifications of DNA can result in such conformational change as observed in the cancer cell DNA and the DNA damaged by ROS. It is well-known that ultraviolet (UV) radiation is carcinogenic and can damage cellular DNA. Exposure to UV light can result in the formation of mutagenic DNA lesions such as cyclobutane pyrimidine dimers (CPD) and (6–4) photoproducts, etc.[56] These lesions can also induce modifications in the structure and thereby the conformation of DNA. Figure 3C shows the SERS spectra, between 575 cm^{-1} and 1550 cm^{-1}, of the healthy and cancer cell DNA before and after exposure to UVC radiation (254 nm for about 1 h). We also monitored the SERS spectra of UVC exposed HaCaT cell DNA as a function of time upon dehydration. Over time, there was no drastic change found in the SERS spectrum of the RB mode of guanine upon dehydration (Figure 3D). The SERS band corresponding to the RB mode of guanine, observed at 652 cm^{-1} remained almost unchanged even after 30 min. Although a small shoulder band was formed after 15 min, the spectra showed a similar trend, as in the case of nonirradiated healthy cell DNA. This suggests that the damage happened in HaCaT cell DNA by the UVC exposure in this case is not capable of any dehydration-induced conformational modification of guanine RB band as in cancer cell DNA. Nevertheless, we noticed that UVC exposure resulted in the modifications in Raman vibrational frequencies of many other vibrations in the cancer and healthy cell DNA (Figure 3). The RB band of cytosine (~785 cm^{-1}) and thymine (795 cm^{-1}), along with complex vibrations of phosphodiester networks, characteristics of B-form DNA backbone geometry, overlapped to form a broad peak at around 804 cm^{-1}. This peak has a lower intensity in nonirradiated healthy and cancer cell DNA, but upon irradiation with UV light, these features are slightly enhanced (Figure 3C). The phosphate backbone conformation marker found at 1086 cm^{-1}, in the healthy cell, was shifted to 1076 cm^{-1} after UV irradiation, while this band observed at 1079 cm^{-1} was slightly shifted to 1076 cm^{-1} upon UV irradiation in cancer cell DNA (Figure 3). The shift in the band for cancer cell DNA suggests a change in the phosphate backbone due to the localized double- or single-strand break. The observed shift in the phosphate backbone band in healthy cell DNA after UV irradiation also confirms this argument. Upon dehydration no drastic difference was observed in this band for healthy cell DNA but it was shifted to 1065 cm^{-1} in the cancer cell DNA (Figure 5). The dehydration-induced modification in the RB band of guanine in HaCaT cell DNA, which is treated with Fenton's reagent, and the absence of the same phenomenon in the DNA separated from UVC exposed HaCaT cells reveal the influence of chemically modified nucleobases in the dehydration-driven modification in Raman bands of nucleobases and it is pointing toward the fact that direct reaction of DNA with Fenton's reagent can easily oxidize the nucleobases.

Compared to the healthy cell DNA, the increased intensity of the symmetric stretching of the ionized phosphate backbone band at 1079 cm^{-1} (Figure 3) in the cancer cell DNA suggests the possibility of Hoogsten-base pairing,[40] indicative of the presence of oxidized guanine. Another noticeable difference is seen in the 1320–1360 cm^{-1} region. In the cancer cell DNA spectrum, the 1349 cm^{-1} band, corresponding to C2′ endo/anti

dx.doi.org/10.1021/ja400187b | J. Am. Chem. Soc. 2013, 135, 4815–4821

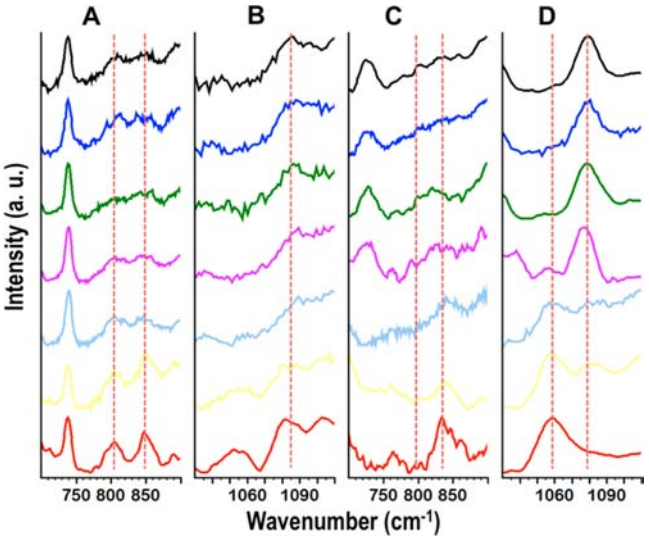

Figure 5. SERS spectra collected as a function of time (top to bottom; 0−30 min; 5 min intervals), showing the stretching vibration of backbone phosphodiester groups and RB vibrations of adenine in healthy (A) and cancer (C) cell DNA. Phosphate backbone marker Raman bands of healthy (B) and cancer (D) cell DNA.

dG conformation, is more prominent than the 1327 cm^{-1} peak, corresponding to the C2′ endo/syn dG conformation (Figure 3).[40] This also suggests a guanine lesion-induced conformational modification in cancer cell DNA.

The intensity of the Raman band found at ∼804 cm^{-1} became more prominent after dehydration, while no considerable difference in intensity was observed in cancer cell DNA (Figure 5A,C). The stretching vibrations corresponding to the backbone phosphodiester marker band in healthy and cancer cell increased in intensity upon dehydration. This feature was found at 848 and 837 cm^{-1} in healthy and cancer cell DNA, respectively (Figure 5A and C). The shift in this marker band, to lower wavenumber in cancer cell DNA, can be due to the possible widening of the groove size due to the increased presence of oxidized base lesions and subsequent modifications in the conformation during dehydration.[22] The intense symmetric stretching of the ionized phosphate band found in cancer cell DNA (Figure 5D) at 1079 cm^{-1} shifted to 1058 cm^{-1} upon dehydration also suggests a change in phosphate backbone due to DNA modification. In healthy cell DNA (Figure 5B), contrary to the cancer cell DNA, this feature was found at 1086 cm^{-1} and remained nearly unaltered upon dehydration.

4. CONCLUSIONS

A simple and reliable method to measure reproducible SERS spectra of DNA, extracted from healthy and cancer cells has been demonstrated. This method provides an easy way to accommodate more DNA molecules in the SERS hot spots, thereby achieving highly distinguishable and reproducible surface enhanced Raman spectra. Using this approach, for the first time, a series of unique conformation-induced formations of DNA Raman marker bands in cancer cell DNA, capable of distinguishing it from the healthy cell DNA, has been monitored as a function of time, upon dehydration. While this method provides easy and reproducible SERS spectra from various DNA, it also offers sufficient information about the lesion-induced conformational changes in DNA, which will certainly be useful for analytical purposes in cancer diagnostics.

■ ASSOCIATED CONTENT

Ⓢ Supporting Information

UV−vis absorption spectra of AgNPs, SERS spectra of various systems such as methylene blue at different experimental conditions, synthetic DNA on different substrates, various synthetic DNA, normal, and oxidized guanosine, and various genomic DNA samples collected as a function of time upon dehydration. These materials are available free of charge via the Internet at http://pubs.acs.org.

■ AUTHOR INFORMATION

Corresponding Author

melsayed@gatech.edu

Notes

The authors declare no competing financial interest.

■ ACKNOWLEDGMENTS

We thank National Science Foundation (NSF) for constantly supporting our research program. This work was supported by NSF-DMR grant.

■ REFERENCES

(1) Benigni, R. *Chem. Rev.* **2005**, *105*, 1767.
(2) Brenner, D. J.; Doll, R.; Goodhead, D. T.; Hall, E. J.; Land, C. E.; Little, J. B.; Lubin, J. H.; Preston, D. L.; Preston, R. J.; Puskin, J. S.; Ron, E.; Sachs, R. K.; Samet, J. M.; Setlow, R. B.; Zaider, M. *Proc. Natl. Acad. Sci. U.S.A.* **2003**, *100*, 13761.
(3) Van Remmen, H.; Ikeno, Y.; Hamilton, M.; Pahlavani, M.; Wolf, N.; Thorpe, S. R.; Alderson, N. L.; Baynes, J. W.; Epstein, C. J.; Huang, T.-T.; Nelson, J.; Strong, R.; Richardson, A. *Physiol. Genomics* **2003**, *16*, 29.
(4) Cooke, M. S.; Evans, M. D.; Dizdaroglu, M.; Lunec, J. *FASEB J.* **2003**, *17*, 1195.
(5) Kang, B.; Mackey, M. A.; El-Sayed, M. A. *J. Am. Chem. Soc.* **2010**, *132*, 1517.
(6) Bernard, P. S.; Wittwer, C. T. *Clin. Chem.* **2002**, *48*, 1178.
(7) Hall, J. G.; Eis, P. S.; Law, S. M.; Reynaldo, L. P.; Prudent, J. R.; Marshall, D. J.; Allawi, H. T.; Mast, A. L.; Dahlberg, J. E.; Kwiatkowski, R. W.; de Arruda, M.; Neri, B. P.; Lyamichev, V. I. *Proc. Natl. Acad. Sci. U.S.A.* **2000**, *97*, 8272.
(8) Jain, P. K.; Huang, X.; El-Sayed, I. H.; El-Sayed, M. A. *Acc. Chem. Res.* **2008**, *41*, 1578.
(9) Huang, X.; El-Sayed, I. H.; Qian, W.; El-Sayed, M. A. *J. Am. Chem. Soc.* **2006**, *128*, 2115.
(10) Ray, P. C. *Angew. Chem., Int. Ed.* **2006**, *45*, 1151.
(11) Stiles, P. L.; Dieringer, J. A.; Shah, N. C.; Van Duyne, R. P. *Annu. Rev. Anal. Chem.* **2008**, *1*, 601.
(12) Nie, S.; Emory, S. R. *Science* **1997**, *275*, 1102.
(13) (a) Alvarez-Puebla, R. A.; Agarwal, A.; Manna, P.; Khanal, B. P.; Aldeanueva-Potel, P.; Carbó-Argibay, E.; Pazos-Pérez, N.; Vigderman, L.; Zubarev, E. R.; Kotov, N. A.; Liz-Marzán, L. M. *Proc. Natl. Acad. Sci. U.S.A.* **2011**, *108*, 8157. (b) He, Y.; Fan, C.; Lee, S.-T. *Nano Today* **2010**, *5*, 282.
(14) Huang, X.; El-Sayed, I. H.; Qian, W.; El-Sayed, M. A. *Nano Lett.* **2007**, *7*, 1591.
(15) Zavaleta, C. L.; Smith, B. R.; Walton, I.; Doering, W.; Davis, G.; Shojaei, B.; Natan, M. J.; Gambhir, S. S. *Proc. Natl. Acad. Sci. U.S.A.* **2009**, *106*, 13511.
(16) Mathew, A.; Sajanlal, P. R.; Pradeep, T. *Angew. Chem., Int. Ed.* **2012**, *51*, 9596.
(17) Papadopoulou, E.; Bell, S. E. J. *Angew. Chem., Int. Ed.* **2011**, *50*, 9058.

(18) Barhoumi, A.; Zhang, D.; Halas, N. J. *J. Am. Chem. Soc.* **2008**, *130*, 14040.
(19) Cooke, M. S.; Evans, M. D.; Dizdaroglu, M.; Lunec, J. *FASEB. J.* **2003**, *17*, 1195.
(20) Yih, J. N.; Chiu, K. C.; Chien, F. C.; Chen, W. Y.; Chen, S. J. *Proc. SPIE.* **2006**, 609906.
(21) Sanchez-Cortes, S.; Berenguel, R. M.; Madejón, A.; Pérez-Méndez, M. *Biomacromolecules* **2002**, *3*, 655.
(22) Movileanu, L.; Benevides, J. M.; Thomas, G. J. *J. Raman Spectrosc.* **1999**, *30*, 637.
(23) Puppels, G. J.; Otto, C.; Greve, J.; Robert-Nicoud, M.; Arndt-Jovin, D. J.; Jovin, T. M. *Biochemistry* **1994**, *33*, 3386.
(24) Thomas, G. J., Jr.; Benevides, J. M.; Overman, S. A.; Ueda, T.; Ushizawa, K.; Saitoh, M.; Tsuboi, M. *Biophys. J.* **1995**, *68*, 1073.
(25) Johnson, R. P.; Richardson, J. A.; Brown, T.; Bartlett, P. N. *J. Am. Chem. Soc.* **2012**, *134*, 14099.
(26) Abell, J. L.; Garren, J. M.; Driskell, J. D.; Tripp, R. A.; Zhao, Y. *J. Am. Chem. Soc.* **2012**, *134*, 12889.
(27) Huser, T.; Orme, C. A.; Hollars, C. W.; Corzett, M. H.; Balhorn, R. *J. Biophotonics* **2009**, *2*, 322.
(28) Haka, A. S.; Shafer-Peltier, K. E.; Fitzmaurice, M.; Crowe, J.; Dasari, R. R.; Feld, M. S. *Proc. Natl. Acad. Sci. U.S.A.* **2005**, *102*, 12371.
(29) (a) Shanmugasundaram, M.; Puranik, M. *Phys. Chem. Chem. Phys.* **2011**, *13*, 3851. (b) Duguid, J. G.; Bloomfield, V. A.; Benevides, J. M.; Thomas, G. J., Jr *Biophys. J.* **1995**, *69*, 2623.
(30) Turkevich, J.; Stevenson, P. C.; Hillier, J. *Discuss. Faraday Soc.* **1951**, *11*, 55.
(31) Besaratinia, A.; Synold, T. W.; Xi, B.; Pfeifer, G. P. *Biochemistry* **2004**, *43*, 8169.
(32) Besaratinia, A.; Synold, T. W.; Chen, H.-H.; Chang, C.; Xi, B.; Riggs, A. D.; Pfeifer, G. P. *Proc. Natl. Acad. Sci. U.S.A.* **2005**, *102*, 10058.
(33) Wei, H.; Cai, Q.; Rahn, R. O. *Carcinogenesis* **1996**, *17*, 73.
(34) Gregory, S. G.; Barlow, K. F.; McLay, K. E.; Kaul, R.; Swarbreck, D.; Dunham, A.; Scott, C. E.; Howe, K. L.; Woodfine, K.; Spencer, C. C. A.; Jones, M. C.; Gillson, C.; Searle, S.; Zhou, Y.; Kokocinski, F.; McDonald, L.; Evans, R.; Phillips, K.; Atkinson, A.; Cooper, R.; Jones, C.; Hall, R. E.; Andrews, T. D.; Lloyd, C.; Ainscough, R.; Almeida, J. P.; Ambrose, K. D.; Anderson, F.; Andrew, R. W.; Ashwell, R. I. S.; Aubin, K.; Babbage, A. K.; Bagguley, C. L.; Bailey, J.; Beasley, H.; Bethel, G.; Bird, C. P.; Bray-Allen, S.; Brown, J. Y.; Brown, A. J.; Buckley, D.; Burton, J.; Bye, J.; Carder, C.; Chapman, J. C.; Clark, S. Y.; Clarke, G.; Clee, C.; Cobley, V.; Collier, R. E.; Corby, N.; Coville, G. J.; Davies, J.; Deadman, R.; Dunn, M.; Earthrowl, M.; Ellington, A. G.; Errington, H.; Frankish, A.; Frankland, J.; French, L.; Garner, P.; Garnett, J.; Gay, L.; Ghori, M. R. J.; Gibson, R.; Gilby, L. M.; Gillett, W.; Glithero, R. J.; Grafham, D. V.; Griffiths, C.; Griffiths-Jones, S.; Grocock, R.; Hammond, S.; Harrison, E. S. I.; Hart, E.; Haugen, E.; Heath, P. D.; Holmes, S.; Holt, K.; Howden, P. J.; Hunt, A. R.; Hunt, S. E.; Hunter, G.; Isherwood, J.; James, R.; Johnson, C.; Johnson, D.; Joy, A.; Kay, M.; Kershaw, J. K.; Kibukawa, M.; Kimberley, A. M.; King, A.; Knights, A. J.; Lad, H.; Laird, G.; Lawlor, S.; Leongamornlert, D. A.; Lloyd, D. M. *Nature* **2006**, *441*, 315.
(35) Petrovykh, D. Y.; Pérez-Dieste, V.; Opdahl, A.; Kimura-Suda, H.; Sullivan, J. M.; Tarlov, M. J.; Himpsel, F. J.; Whitman, L. J. *J. Am. Chem. Soc.* **2005**, *128*, 2.
(36) Cho, W. J.; Kim, Y.; Kim, J. K. *ACS Nano* **2011**, *6*, 249.
(37) Hatab, N. A.; Hsueh, C.-H.; Gaddis, A. L.; Retterer, S. T.; Li, J.-H.; Eres, G.; Zhang, Z.; Gu, B. *Nano Lett.* **2010**, *10*, 4952.
(38) Deng, H.; Bloomfield, V. A.; Benevides, J. M.; Thomas, G. J. *Biopolymers* **1999**, *50*, 656.
(39) Dickerson, R. E.; Drew, H. R. *Proc. Natl. Acad. Sci. U.S.A.* **1981**, *78*, 7318.
(40) Pagba, C. V.; Lane, S. M.; Wachsmann-Hogiu, S. *Biomed. Opt. Exp.* **2011**, *2*, 207.
(41) Klaunig, J. E.; Kamendulis, L. M. *Annu. Rev. Pharmacol. Toxicol.* **2004**, *44*, 239.
(42) Escodd, A.; Gedik, C. M.; Collins, A. *FASEB J.* **2005**, *19*, 82.
(43) Dickerson, R. E.; Drew, H. R. *Proc. Natl. Acad. Sci. U.S.A.* **1981**, *78*, 7318.
(44) Miller, J. H.; Fan-Chiang, C.-C. P.; Straatsma, T. P.; Kennedy, M. A. *J. Am. Chem. Soc.* **2003**, *125*, 6331.
(45) NaÔmé, A.; Schyman, P.; Laaksonen, A.; Vercauteren, D. P. *J. Phys. Chem. B* **2010**, *114*, 4789.
(46) Pal, S. K.; Zhao, L.; Zewail, A. H. *Proc. Natl. Acad. Sci. U.S.A.* **2003**, *100*, 8113.
(47) Sokolov, A. P.; Grimm, H.; Kahn, R. *J. Chem. Phys.* **1999**, *110*, 7053.
(48) Kistner, C.; Andre, A.; Fischer, T.; Thoma, A.; Janke, C.; Bartels, A.; Gisler, T.; Maret, G.; Dekorsy, T. *Appl. Phys. Lett.* **2007**, *90*, 233902.
(49) Barone, F.; Lankas, F.; Spackova, N.; Sponer, J.; Karran, P.; Bignami, M.; Mazzei, F. *Biophys. Chem.* **2005**, *118*, 31.
(50) Beard, W. A.; Batra, V. K.; Wilson, S. H. *Mutat. Res. Genet. Toxicol. Environ. Mutagen.* **2010**, *703*, 18.
(51) Singh, S. K.; Szulik, M. W.; Ganguly, M.; Khutsishvili, I.; Stone, M. P.; Marky, L. A.; Gold, B. *Nucleic Acids Res.* **2011**, *39* (15), 6789–6801.
(52) Faucher, F.; Doublié, S.; Jia, Z. *Int. J. Mol. Sci.* **2012**, *13*, 6711.
(53) White, B.; Smyth, M. R.; Stuart, J. D.; Rusling, J. F. *J. Am. Chem. Soc.* **2003**, *125*, 6604.
(54) Henle, E. S.; Linn, S. *J. Biol. Chem.* **1997**, *272*, 19095.
(55) Pinak, M. *J. Mol. Struct.–THEOCHEM* **2002**, *583*, 189.
(56) Sinha, R. P.; Hader, D.-P. *Photochem. Photobiol. Sci.* **2002**, *1*, 225.